

Rice Area Determination Using Landsat-Based Indices and Land Surface Temperature Values

Burçin Saltık, Levent Genç

Abstract—In this study, it was aimed to determine a route for identification of rice cultivation areas within Thrace and Marmara regions of Turkey using remote sensing and GIS. Landsat 8 (OLI-TIRS) imageries acquired in production season of 2013 with 181/32 Path/Row number were used. Four different seasonal images were generated utilizing original bands and different transformation techniques. All images were classified individually using supervised classification techniques and Land Use Land Cover Maps (LULC) were generated with 8 classes. Areas (ha, %) of each classes were calculated. In addition, district-based rice distribution maps were developed and results of these maps were compared with Turkish Statistical Institute (TurkSTAT; TSI)'s actual rice cultivation area records. Accuracy assessments were conducted, and most accurate map was selected depending on accuracy assessment and coherency with TSI results. Additionally, rice areas on over 4° slope values were considered as mis-classified pixels and they eliminated using slope map and GIS tools. Finally, randomized rice zones were selected to obtain maximum-minimum value ranges of each date (May, June, July, August, September images separately) NDVI, LSWI, and LST images to test whether they may be used for rice area determination via raster calculator tool of ArcGIS. The most accurate classification for rice determination was obtained from seasonal LSWI LULC map, and considering TSI data and accuracy assessment results and mis-classified pixels were eliminated from this map. According to results, 83151.5 ha of rice areas exist within study area. However, this result is higher than TSI records with an area of 12702.3 ha. Use of maximum-minimum range of rice area NDVI, LSWI, and LST was tested in Meric district. It was seen that using the value ranges obtained from July imagery, gave the closest results to TSI records, and the difference was only 206.4 ha. This difference is normal due to relatively low resolution of images. Thus, employment of images with higher spectral, spatial, temporal and radiometric resolutions may provide more reliable results.

Keywords—Landsat 8 (OLI-TIRS), LULC, spectral indices, rice.

I. INTRODUCTION

RICE is one of the most important crops for more than three million people [1], and can be produced in many areas of the world. However, the major part of rice (90%) is produced in Asia [2]. On the other hand, researchers reported that many countries import rice since the supply is not enough to meet the demand [3], [4]. Thus, determination of rice

growing areas within the production season provides to foreseen the amount of rice to be imported.

The rice cultivated area determination via traditional methods is laborious, time consuming, and less precise [2]. Moreover, the results became available months after production season ends. On this account, using practicable techniques which provide rapid, reliable, and relatively economic results for provisions allow planners and decision-makers to estimate the amount of production before harvest. In this context, use of satellite imageries for this purpose has become an important concern. However, using images with low/mediate temporal/spatial resolutions may have some disadvantages. On the other hand, rice has specific spectral reflectance characteristics and it is easy to distinguish from other land cover types [5]-[7].

In present study, it was aimed to evaluate performances of different image pre-processing techniques to determine rice areas within Thrace and Marmara regions, and test the use of raw values of indices for rice area determination in pilot area. To achieve these aims Landsat 8 (OLI-TIRS) images, GIS, and ancillary data were used in the study.

II. MATERIALS AND METHODS

A. Study Area

Study was conducted around the main rice cultivation areas [8], located within the Thrace and South-Marmara regions of Turkey. It was reported that more than 60% of Turkey's total rice is produced in this area [8]. The study area was restricted with Landsat scene coverage (181/32 Path/Row number). Fig. 1 shows the location of study area [9]. Main settlements within the study area are Balıkesir, Çanakkale, Edirne, and Tekirdag provinces and their districts.

B. Remote Sensing Data & Pre-processing

In present study, Landsat 8 (OLI-TIRS) imageries with 181/32 P/R number were used to determine LULC status. Images were freely downloaded from USGS website. The image acquisition dates within the production season (May-September, M-S) of 2013 are given in Table I.

Performances of seasonal (M-S) images of original bands, Land Surface Temperature (LST), Normalized Difference Vegetation Index (NDVI), and Land Surface Water Index (LSWI) to discriminate rice areas from other LULC types were evaluated. M-S-ORIGINAL was generated using original 2nd-7th bands of five single-date images, including a total of 30-bands (M-S-ORIGINAL) (1). Seasonal NDVI (M-S-NDVI), seasonal LSWI (M-S-LSWI), and seasonal LST (M-S-LST) images were obtained via (2)-(9). Fig. 2 illustrates the

Burçin Saltık was with Çanakkale Onsekiz Mart University, Faculty of Agriculture, Department of Agricultural Structures & Irrigation, Agricultural Sensors and Remote Sensing Lab. (ASRESEL) Çanakkale, 17020, Turkey

Levent Genç* is the corresponding author with Çanakkale Onsekiz Mart University, Faculty of Architecture and Design, Department of Urban & Regional Planning, Land Use and Climate Change Lab. (LUCC-LAB) Çanakkale, 17020, Turkey. (corresponding author to provide phone: 286-218-0018-3032; e-mail: leventgc@comu.edu.tr).

* This research was based on a part of Burçin Saltık's M.Sc. thesis.

steps for generating images to be used in LULC classification.
Generated seasonal images can be seen on Figs. 4-7.

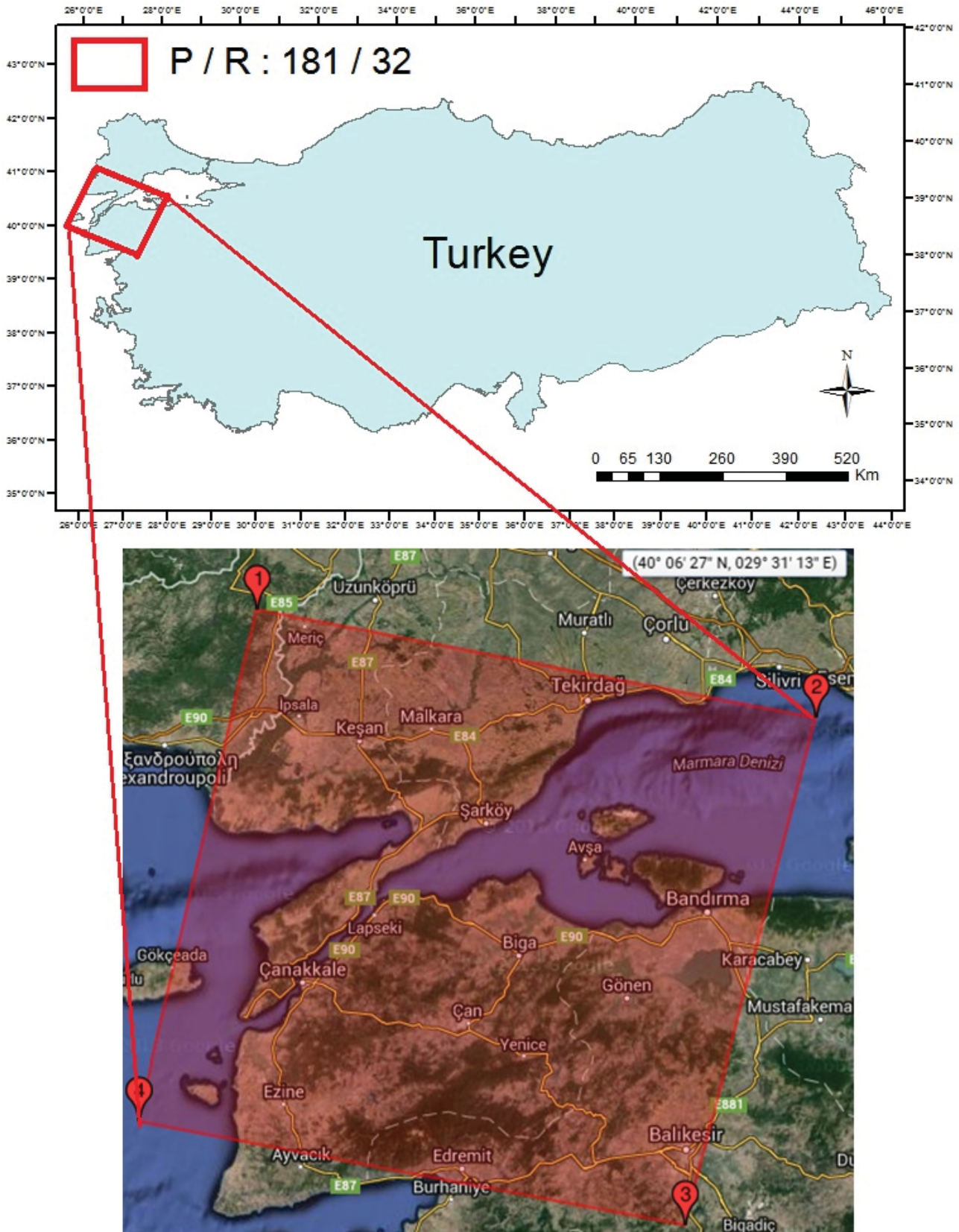


Fig. 1 Study area

TABLE I
ACQUISITION DATES OF THE IMAGES

Day	Month	Month Abbreviation	Year
18	May	M	2013
19	June	JN	2013
21	July	JL	2013
22	August	A	2013
07	September	S	2013

$$M - S - ORIGINAL = 2^{nd} + \dots + 7^{th} (M + JN + JL + A + S) \quad (1)$$

$$NDVI = \frac{(NIR-RED)}{(NIR+RED)} \quad (2)$$

$$M - S - NDVI = NDVI (M + JN + JL + A + S) \quad (3)$$

$$LSWI = \frac{(NIR-SWIR)}{(NIR+SWIR)} \quad (4)$$

$$M - S - LSWI = LSWI (M + JN + JL + A + S) \quad (5)$$

$$L = L_{min} + (L_{max} - L_{min}) \times \left(\frac{DN}{2^{n-1}}\right) \quad (6)$$

$$T_B (^{\circ}K) = \frac{K_2}{\ln\left(\frac{K_1}{L} + 1\right)} \quad (7)$$

$$T_B (^{\circ}C) = T_B (^{\circ}K) - 273 \quad (8)$$

$$M - S - LST = LST (M + JN + JL + A + S) \quad (9)$$

where; *NIR*: Near infrared band of each single-date image; *RED*: Red band of each single-date image; *SWIR*: Short wave infrared band of each single-date image; *Lmin*: Spectral radiance of DN value 1; *Lmax*: Spectral radiance of DN value (2^n-1); *n*: Radiometric resolution of image; *K₁*: Calibration constant 1; *K₂*: Calibration constant 2; *T_B*: Surface temperature.

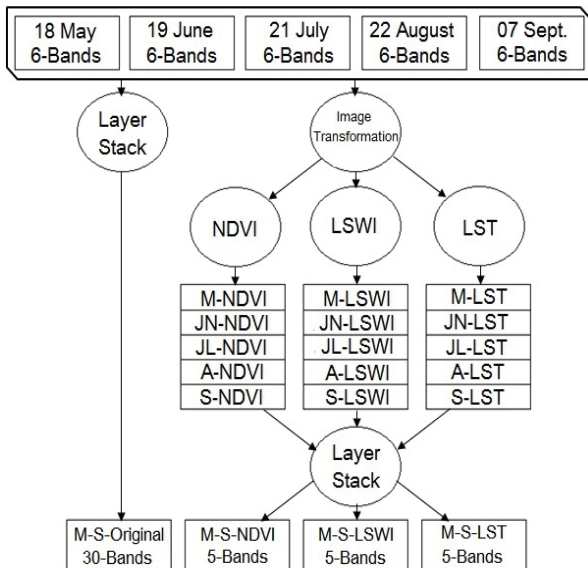


Fig. 2 Generation of the seasonal imagery for LULC determination

Fig. 3 summarizes the rice determination route applied in the study. The details of the processes are explained in further sections of the paper.

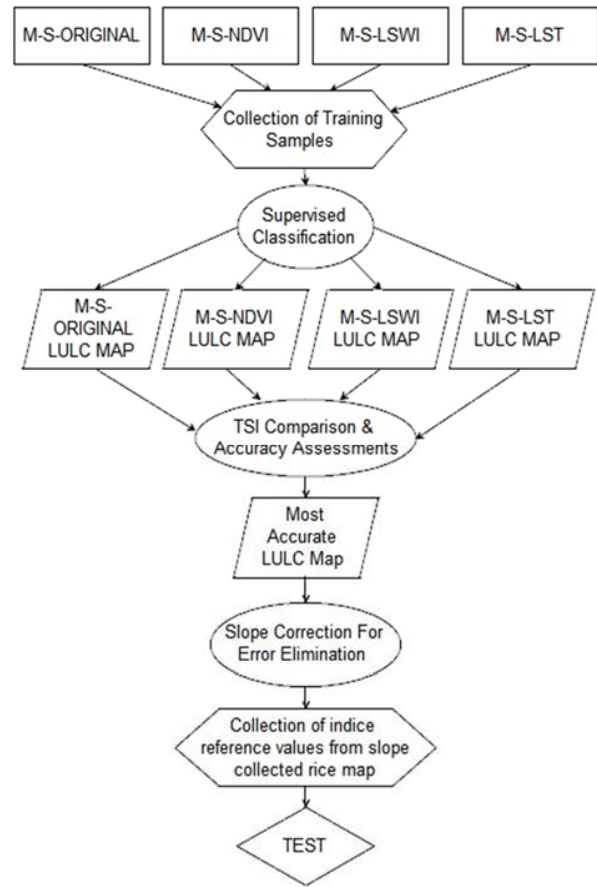


Fig. 3 Rice determination route

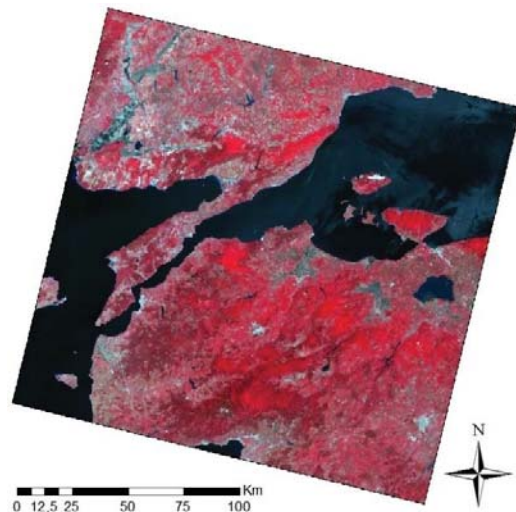


Fig. 4 M-S-Original image (30-Band)

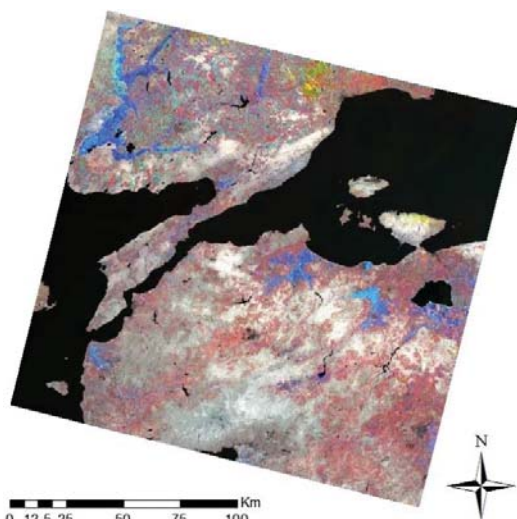


Fig. 5 M-S-NDVI image (5-Band)

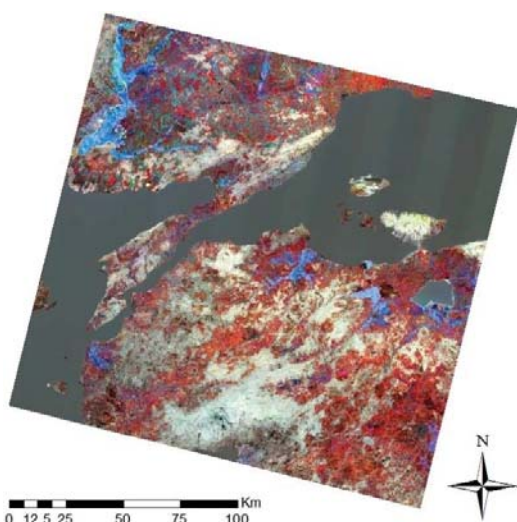


Fig. 6 M-S-LSWI image (5-Band)

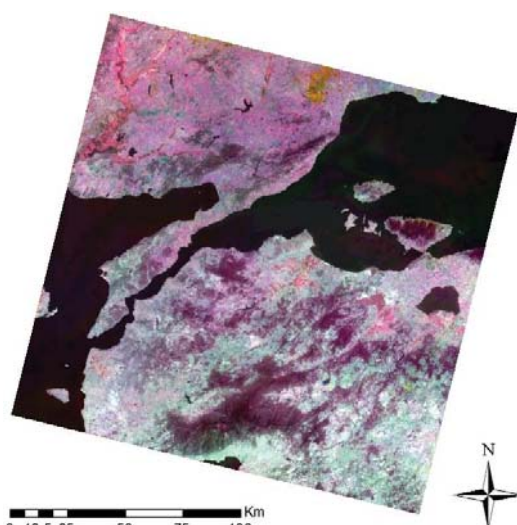


Fig. 7 M-S-LST image (5-Band)

C. LULC Map Generation & Accuracy Assessment

Since rice cultivated areas are one of the components of LULC maps within a specific area, they can be determined via classification techniques. All images were classified using supervised classification maximum likelihood algorithm to generate LULC maps. Erdas Imagine (2011) software was used for image classification. Same training samples were used for each classification process.

Eight main classes were selected to be included in the maps; Rice, Forest, Grazing Land, Olive Tree, Other Fruit Tree, Other Agricultural Land, Water Surface, and Residential Area-Bare Soil. Neighbourhood analyses (3x3 pixels) were applied to classified image. The areas of each class were calculated in hectares (ha), and percentages (%). However, only the rice-related results are shown in present study.



Fig. 8 Boundaries of the districts located in the study area

Accuracy assessments were conducted to determine the reliability of the maps. In this step, accuracy of 240 points were checked utilizing Google Earth application (Fig. 9). Typically, accuracy reports involve error matrices, the reference totals (RT), classified totals (CT), number of corrects (NC), producers' accuracy % (PA), users' accuracy % (UA), Kappa statistics (K) for each class, and overall classification accuracy % (CA) and overall Kappa statistics (OK). Kappa statistic is accepted as a key indicator for the coherence of overall or class-dependent accuracies. Kappa value over 0.80 for a given class or overall classification designates the acceptable.

Prior to accuracy assessments, LULC maps were trimmed according to Turkish Administrative Units boundaries (Fig. 8). District boundaries were also used for generating rice distribution maps, so district-based rice areas could be

calculated, and compared with district-based TSI records. According to this comparison, LULC map with closest result to TSI and also Kappa value over 0.80, was selected for further analyses.

The most accurate rice distribution map was selected to be used in further analysis depending on the best TSI relations and coherent accuracy assessment results.

D. Elimination of Potential Rice Classification Errors

As it is reported in the literature, rice cultivation on lands with slope value over 4° may not be economic and it may be

difficult to obtain high yield [10]. On this account, the rice class of selected LULC map was evaluated depending on the appropriate slope range. Shuttle Radar Topography Mission (SRTM) DEM was used to derive slope map [9]. Rice areas with slope over 4° are considered as potential rice classification errors, and eliminated from rice distribution map (Fig. 10). Whole process was conducted using ArcGIS (10.3) software. Final results are compared with TSI data to evaluate whether the process provided more reliable results.

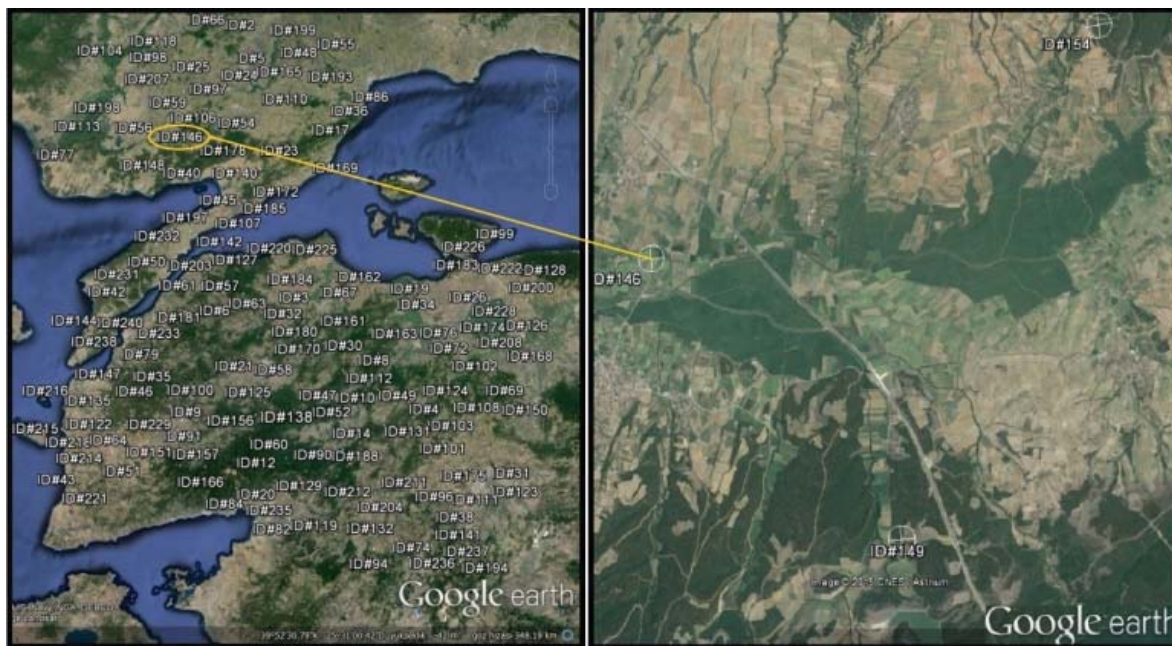


Fig. 9 Representation of accuracy assessments

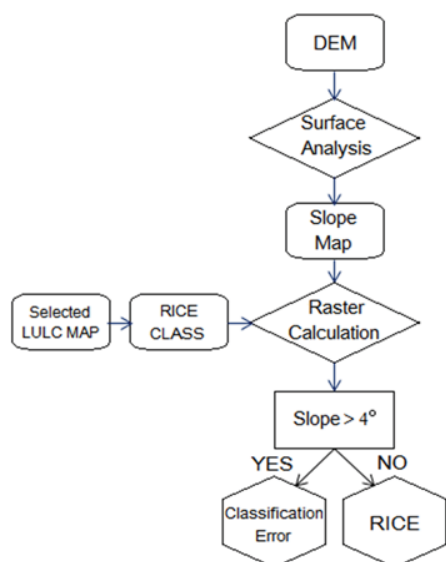


Fig. 10 Schematic representation of classification error removal

E. Sample Zones & Spatial Analysis

Previous analyses were conducted to determine LULC patterns, especially rice class locations to decide where to

draw spectral rice samples, since there was any spatial rice distribution map. Subsequent to the selection of accurate rice distribution map, sample zones were randomly sited, and descriptive statistics of the zones were calculated for all dates and indices. Use of the minimum-maximum value ranges for rice discrimination was tested in Meric district (pilot area) of Edirne province, where rice production is the main agricultural interest. The slope threshold was also used in the spatial analysis (ArcGIS 10.3). Fig. 11 shows the representative illustration of the process.

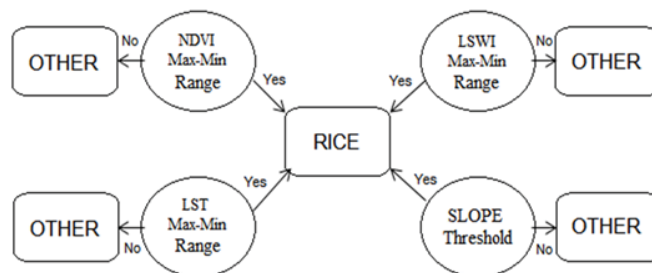


Fig. 11 Rice determination criteria based on max-min ranges

III. RESULTS AND DISCUSSIONS

A. LULC Classification & Rice Distribution Maps

LULC maps were generated using M-S-ORIGINAL, M-S-NDVI, M-S-LSWI, and M-S-LST images. To avoid duplication, only the rice distribution maps were given in this section. Figs. 12-15 represent the district based rice and other classes, respectively. On the other hand, the areas of rice classes in hectares and percentages for each LULC maps are given in Table II. Table II covers the rice class results for whole study area. The white areas outside the 181/32 scene frame contains no information since these areas are out of focus.

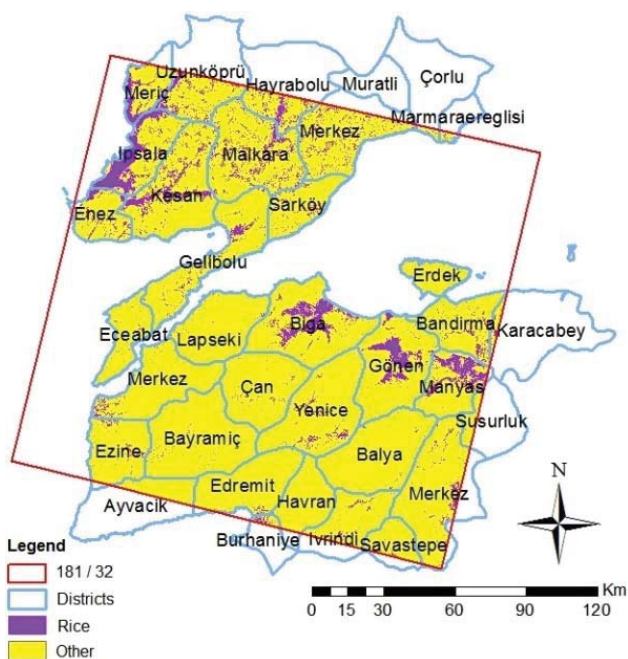


Fig. 12 Rice distribution map (M-S-Original-LULC)

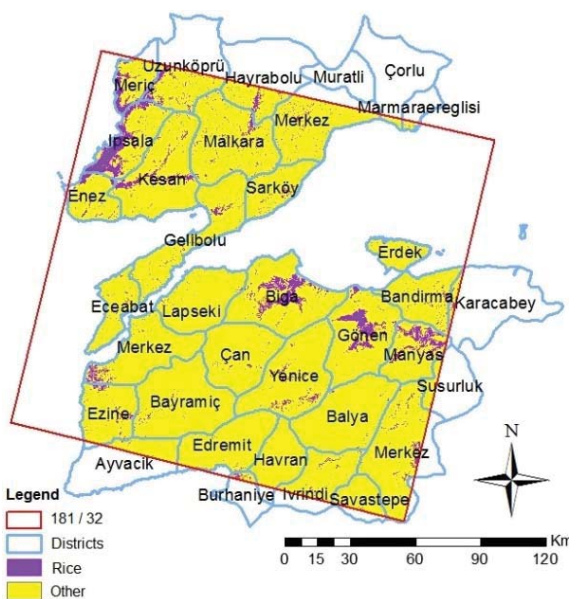


Fig. 13 Rice distribution map (M-S-NDVI-LULC)

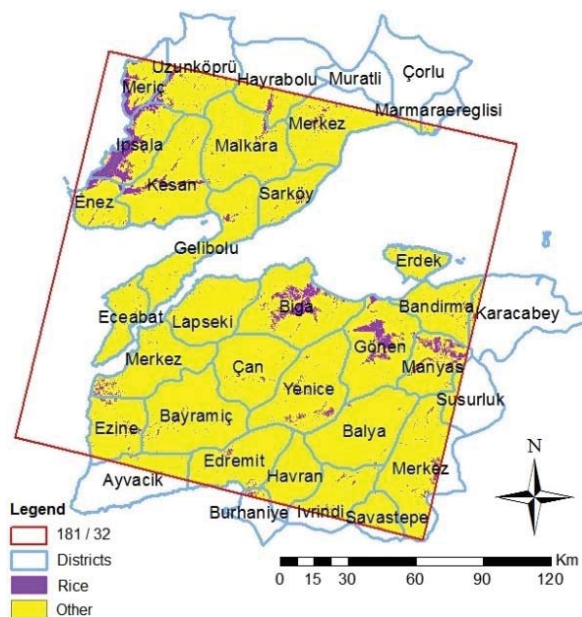


Fig. 14 Rice distribution map (M-S-LSWI-LULC)

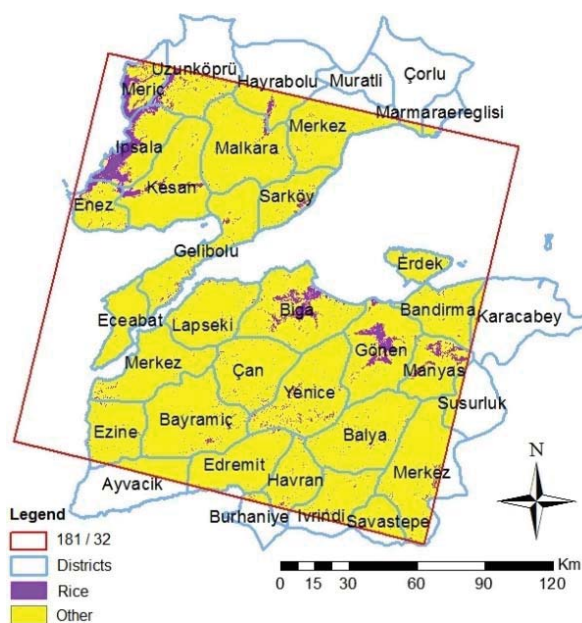


Fig. 15 Rice distribution map (M-S-LST-LULC)

LULC Map	Area (ha)	Area (%)
M-S-ORIGINAL	199792.2	9.0
M-S-NDVI	141828.8	6.4
M-S-LSWI	121851.0	5.5
M-S-LST	124955.4	5.6

According to M-S-ORIGINAL LULC map, the portion of rice areas within whole study area is found to be 9.0%. Moreover, portion of rice areas for the M-S-NDVI derived LULC map was 6.4%. The portions of rice areas for seasonal LSWI and LST LULC maps were almost equal which were 5.5 and 5.6% respectively. However, the difference between

these two was 3104.4 in terms of hectares (ha). On the other hand, there is a great difference between 9.0 and 5.5%. It can be seen that 77941 ha difference occurred between the LULC maps which were included the maximum and the minimum areas for rice. Thus, the importance of determining the most appropriate image for rice determination became more remarkable.

B. Relations between TSI Data & Rice Distributions

Depending on the TSI data, the major producer districts were selected and their actual production statuses were compared with the results of the study. Results demonstrated that the closest results to TSI data were obtained from M-S-LSWI rice distribution map with a R^2 of 0.8626. It was followed by the M-S-NDVI ($R^2=0.8385$). It should be noticed that even though the rice area portions of M-S-LSWI and M-S-LST was very close (5.5 and 5.6%), the district-based distributions were found to be more reliable for M-S-LSWI since the R^2 value was considerably higher. Figs. 16-19 show the relations according to LULC maps.

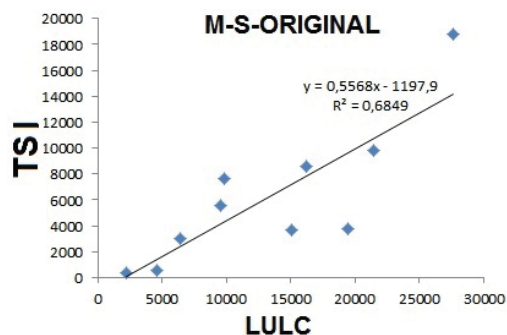


Fig. 16 Relations between TSI and M-S-Original RDM data

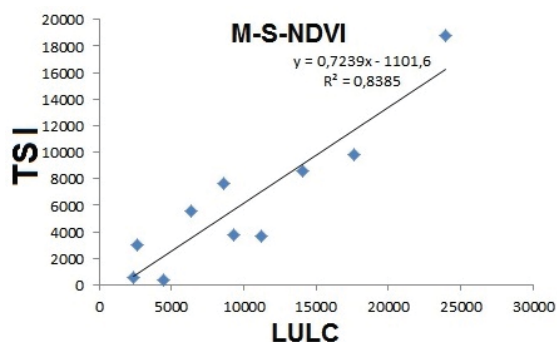


Fig. 17 Relations between TSI and M-S-NDVI RDM data

C. Accuracy Assessments & LULC Map Selection

Typically, error matrices and accuracy reports are composed for each class as results of accuracy assessments. The RT, CT, NC, PA, UA, K for only rice class are sited, whereas CA and OK were given for overall classification in Table III.

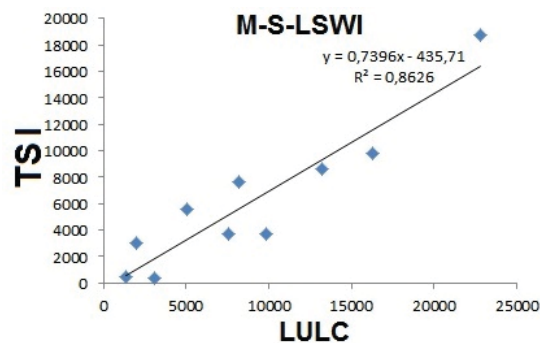


Fig. 18 Relations between TSI and M-S-LSWI RDM data

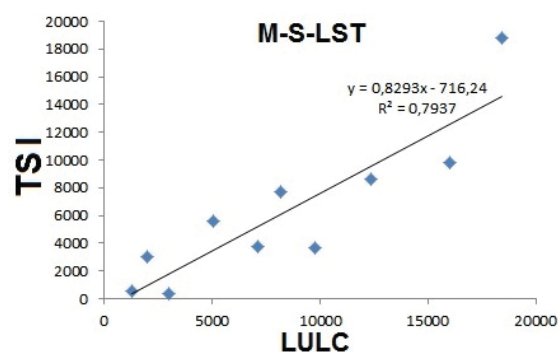


Fig. 19 Relations between TSI and M-S-LST RDM data

TABLE III
 SUMMARY OF ERROR MATRICES & ACCURACY REPORTS

LULC	RT	CT	NC	PA	UA	K	CA	OK
ORIG.	18	24	18	100.0	75.0	0.7297	88.3	0.8486
NDVI	20	20	19	95.0	95.0	0.9455	82.1	0.7731
LSWI	17	19	16	94.1	84.2	0.8301	79.2	0.7346
LST	14	19	12	85.7	63.1	0.6088	71.7	0.6387

As it can be seen on Table III, K statistics related to rice classification of NDVI and LSWI maps are over 0.80 with values of 0.9455 and 0.8301 respectively. Although the M-E-ORIGINAL LULC map has the higher value of CA, the rice classification showed poor results since K for rice is found to be 0.7297. Performance of M-E-LST image was considerably low for overall and rice classification due to the lower values of K statistics as 0.6387 and 0.6088 respectively. On the other hand, both of the seasonal NDVI and LSWI LULC maps showed high-level rice classification performance. However, M-E-LSWI LULC map was selected for further analysis due to the fact that district-based TSI relations gave better results ($R^2=0.8626$).

D. Slope-Corrected Rice Distribution Map

Results of surface analysis indicated that 6875.5 ha (5.6%) rice class were located on lands with slope values higher than the threshold value (4°). These areas were removed from M-S-LSWI rice distribution map using raster calculation tool of ArcGIS software. The final rice distribution map (slope-corrected) is given in Fig. 20. According to this map, 83151.5 ha area were covered by rice class, and this result exceeding TSI records with an area of 12702.3 ha. These differences are considered normal for middle scaled spatial resolution of

Landsat images.

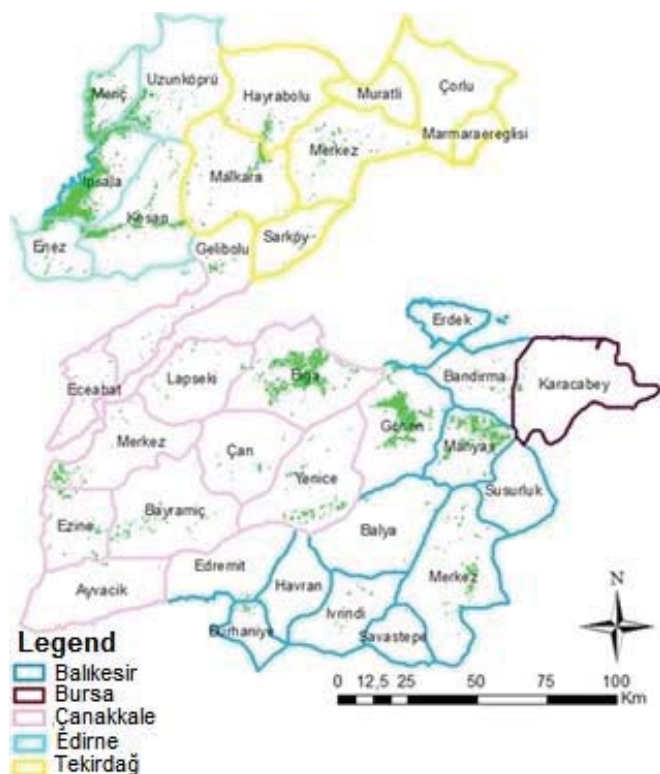


Fig. 20 Slope-Corrected rice distribution map

It is clear that main producer districts are Ipsala, Kesan, Meric and Uzunkopru districts of Edirne province, Provincial center and Biga district of Canakkale province, Gonen and Manyas districts of Balikesir province, and Hayrabolu and Malkara districts of Tekirdag province (Fig. 20). Elimination of rice pixels over inappropriate slope values provided more consisted results for TSI comparisons with a R^2 of 0.9592 (Fig. 21).

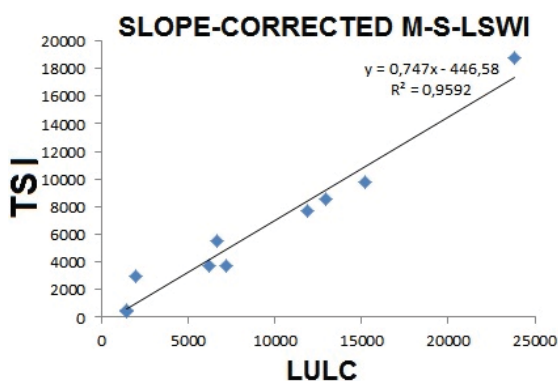


Fig. 21 Relations between TSI and slope corrected M-S-LSWI rice data

E. Selection of Sample Zones & Results of Zonal Statistics

Sample zones were selected from corrected rice distribution map. Representative sample sites on M-S-LSWI LULC map, M-S-NDVI, M-S-LSWI, and M-S-LST can be seen on Figs.

22 (a)-(d). Reference values were determined via zonal statistics, and summarized in Table IV. The use of reference values for rice determination was tested for all single-date images in pilot area.

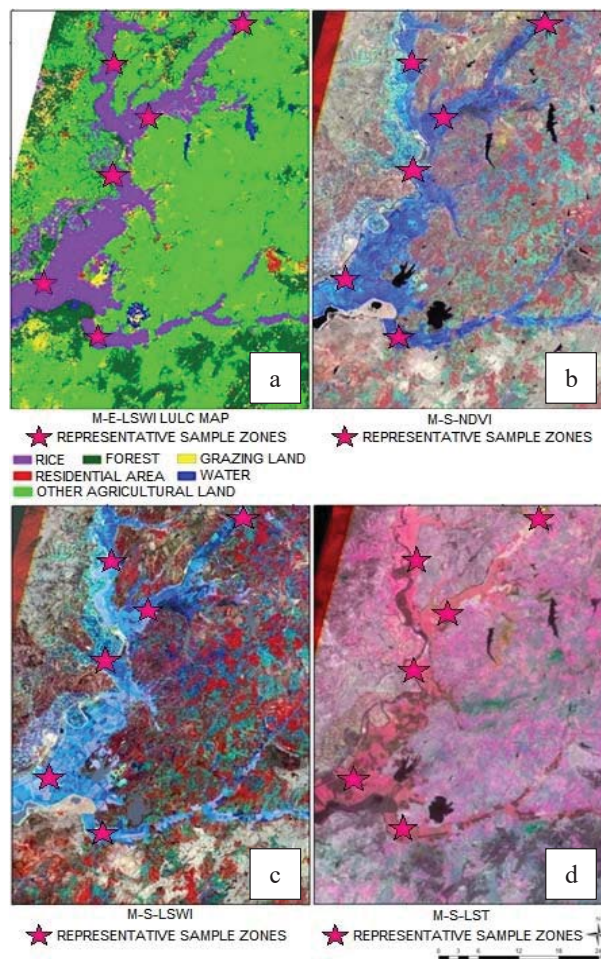


Fig. 22 Collection of reference values via sample zones (a) ME-LSWI LULC Map, (b) M-S-NDVI, (c) M-S-LSWI, (d) M-S-LST

TABLE IV
 SUMMARY OF ERROR MATRICES & ACCURACY REPORTS

M-S Image	Value	DATE OF 2013				
		18 M	19 JN	21 JL	22 JN	07 S
NDVI	Min.	~ -0.050	~ -0.004	~ 0.240	~ 0.404	~ 0.336
	Max.	~ 0.241	~ 0.470	~ 0.600	~ 0.580	~ 0.515
LSWI	Min.	~ -0.113	~ -0.005	~ 0.185	~ 0.209	~ 0.200
	Max.	~ 0.261	~ 0.275	~ 0.379	~ 0.411	~ 0.377
LST	Max.	22	23	21	20	20
	Max.	35	27	28	23	23

Use of NDVI, LSWI, LST reference values and slope threshold for rice area determination was investigated to assess whether rice areas can be determined via simultaneous use of mentioned indices. As it can be recognized from Fig. 10, if the NDVI, LSWI, LST and slope values of a given pixel are within the max.-min. ranges, the pixel nominated as "RICE", otherwise "OTHER". The effectuality of this assumption was tested in Meric district for all dates (ArcGIS

10.3) (Fig. 23 (a)). Moreover, results of the analysis are compared with the ones obtained from slope-corrected rice distributions (Figs. 23 (a), (b)).

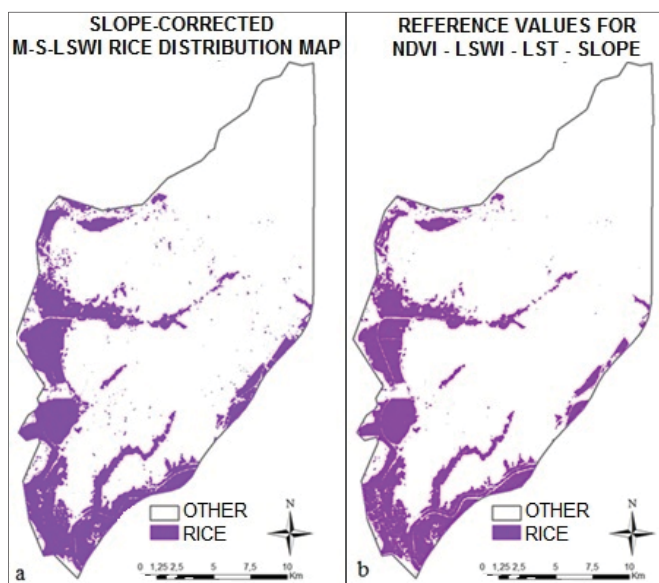


Fig. 23 Comparison of the results for pilot area (a) Slope-Corrected M-S-LSWI rice distribution map, (b) Rice area map obtained via reference values for NDVI-LSWI-SLT-Slope images of 21 July image

Within all date images, 21 July 2013 image gave the closest result. GIS analysis results showed that 8204.4 ha of rice areas were determined according to slope-corrected rice distributions in Meric district (Fig. 23 (a)). However, 7888.4 ha rice area were found via GIS analysis using NDVI, LSWI, LST and slope reference values together (Fig. 23 (b)). In comparison with classification results (Fig. 23 (a)), GIS analysis gave more similar results to actual rice status (Fig. 23 (b)); there is 7682 ha rice cultivated areas in Meric according to TSI record. Observation of better fitted results is thought to be sourced from simultaneously used of all parameters. The difference between analysis results and TSI rice area was only 206.4 ha which was normal for LULC studies conducted using images with middle spatial resolution like Landsat. Using higher resolution images are strongly suggested for more accurate results for precise studies.

IV. CONCLUSION

In this study, seasonal M-S-ORIGINAL, NDVI, LSWI, and LST images were generated using monthly acquired Landsat images. Images were used to determine rice areas within study area, which is covered by 181/32 Landsat scene. District boundaries were used as ancillary data for generation of rice distribution maps. Most congruent rice distribution map was selected depending on the accuracy assessments and coherency with TSI records. M-S-LSWI LULC_{RICE} map have presented better performance compared to the rest maps and the calculated rice area was 83151.5 ha. Rice pixels on lands located over 4° slope were accepted as classification error and

removed from this map. The extent of removed rice areas were 6875.5 ha. The final map gave better-fitted results with TSI records ($R^2=0.9592$). Sample rice zones were sited to collect reference values of NDVI, LSWI, and LST to test the usability of references for rice determination in test site (Meric district). The 21 July image showed the best performance for rice determination and 7888.4 ha and the difference was found to be 206.4 ha, which can be tolerated in error limits for such studies conduction using middle resolution images.

REFERENCES

- [1] G. Khush, "What it will take to Feed 5.0 Billion Rice Consumers in 2030", *Plant Molecular Biology*, vol. 59, pp. 1-6, 2005.
- [2] M. K. Mohles, Q. K. Hassan, and E. H. Chowdhuri, "Application of Remote Sensors in Mapping Rice Area and Forecasting Its Production: A Review", *Sensors*, vol. 15, pp. 769-791, 2015.
- [3] M. Purevdorj, and M. Kubo, "The Future of Rice Production, Consumption and Seaborne Trade: Synthetic Prediction Method", *J. Food Distrib. Res.*, vol. 36, pp. 250-259, 2005.
- [4] B. Sade, S. Soylu, I. Sezer, N. Başer, H. Sürük, M. Şahin, and T. Yetiş. "Ulusal Hububat Konseyi Çeltik Raporu", Konya, Turkey, 2011 (In Turkish).
- [5] T. Bukhari, W. Takken, A. Githeko, and J. M. C. Koenraadt, "Efficacy of Aquatoin, a Monomolecular Film, for the Control of Malaria Vectors in Rice Paddies", *PLoS ONE*, vol. 6, no. 6, pp. 1-13, 2011.
- [6] I.W. Nuarsa, F. Nishio, and C. Hongo, "Spectral Characteristics and Mapping of Rice Plants Using Multi-Temporal Landsat Data", *Journal of Agricultural Science*, vol. 3, no. 1, pp. 54-67, 2011.
- [7] X. Xiao, S. Boles, S. Frohling, W. Salas, B. Moore, and C. Li, "Landscape-scale Characterization of Cropland in China Using Vegetation and Landsat TM Images", *International Journal of Remote Sensing*, vol. 23, pp. 3579 - 3594, 2002.
- [8] TurkSTAT, Turkish Statistical Institute, 2015, <http://turkstat.gov.tr>
- [9] USGS, United States Geological Survey, 2016, <http://earthexplorer.usgs.gov>
- [10] Eraslan, "Tosya'da Çeltik (*Oryza sativa* L.) Tarımı", 2012 (In Turkish) <http://www.ttae.gov.tr>